Hydration of the Chloride Ion in Concentrated Aqueous Solutions using Neutron Scattering and Molecular Dynamics

Eva Pluhařová,[1] *Henry E. Fischer,*[2] *Philip E. Mason,*[1*] *and Pavel Jungwirth*[1*]

[1]Institute of Organic Chemistry and Biochemistry, Academy of Sciences of the Czech Republic, Flemingovo nám. 2, 16610 Prague 6, Czech Republic

[2]Institut Laue-Langevin, 6 rue Jules Horowitz, B.P. 156, 38042 Grenoble cedex 9, France

[*]Corresponding authors: phil.mason@uochb.cas.cz (PEM) and pavel.jungwirth@uochb.cas.cz (PJ)

KEYWORDS, chloride, lithium, neutron scattering, molecular dynamics, solution.

Abstract

Neutron scattering experiments were performed on 6m LiCl solutions in order to obtain the solvation structure around the chloride ion. Molecular dynamics simulations on systems mirroring the concentrated electrolyte conditions of the experiment were carried out with a variety of chloride force fields. In each case the simulations were run with both full ionic charges and employing the electronic continuum correction (implemented through charge scaling) to account effectively for electronic polarization. The experimental data were then used to assess the successes and shortcomings of the investigated force fields. We found that due to the very good signal to noise ratio in the experimental data, they provide a very narrow window for the position of the first hydration shell of the chloride ion. This allowed us to establish the importance of effectively accounting for electronic polarization, as well as adjusting the ionic size, for obtaining a force field which compares quantitatively to the experimental data. The present results emphasize the utility of performing neutron diffraction with isotopic substitution as a powerful tool in gaining insight and examining the validity of force fields in concentrated electrolyte solutions.

Introduction

Either by mass, or by number of ions, chloride is the most common aqueous ion on Earth. In the Earth crust, chloride is one or two orders of magnitude less abundant than sodium,[1] yet interestingly in the oceans the two ions occur in almost equal proportions.[2] Of the liquid water on the earth, about 97 % of it exists in the oceans as an electrolyte of which chloride is the most abundant ion by mass. Chloride is also an important ion in biochemistry. In humans the concentration of chloride is about an order of magnitude lower than it is in seawater (approximately 0.2% by mass vs. 2 % by mass). Given this pervasive nature of the chloride ion, it is not surprising that a lot of work has been done on the hydration of the chloride ion at the molecular level. This encompasses quantum mechanical[3] and molecular dynamics studies[4] as well as numerous experimental studies including both X-ray[5] and neutron scattering studies.[6]

In recent decades, molecular dynamics (MD) has emerged as a powerful predictive and interpretive tool in modern chemistry and biochemistry, in particular in combination with microscopic structural data on which the accuracy of such models can be tested. For this purpose, data from diffraction experiments are generally preferred over spectroscopic data as they provide a more direct measure of the structure of the solution. Structural data on these systems can be obtained by either neutron scattering or X-ray diffraction. Of these two, neutron scattering has a vastly superior ability to resolve hydrogen nuclei, which tend to be almost invisible in X-ray scattering due to the low number of electrons of the hydrogen atoms.[7,8] Measuring the total neutron scattering pattern from a solution is of limited use for a simple aqueous electrolyte since the measurement is a convolution of 10 partial structure factors (HH, HO, HM, HX, OO, OM, OX, MM, MX, and XX where M is the cation and X is the anion).[7] Using the technique of Neutron Scattering with Isotopic Substitution (NDIS), one can reduce these 10 correlations to 4 (XH, XO, XM, and XX, where X is the isotopically substituted nucleus – anion in this case).[9] This technique requires measurement of total neutron scattering patterns from two chemically identical solutions which vary only in the isotopic concentration of the substituted nucleus (chloride in the present study). From the

difference of these two scattering patterns it is possible to obtain the structure of the solution around the substituted chloride nuclei.

NDIS has been used to examine the structure of the chloride ion in different solutions.[6,10] The contrast in a NDIS experiment is almost linearly proportional to the concentration of the solution; the higher the concentration of the solution, the better the signal to noise ratio in the experimental measurement is. Lithium chloride makes a good topic of study here as it is the most soluble (up to ~10 molal) of the alkali metal chlorides.[11] At the highest concentration there are only ~2.5 water molecules per ion. In this study a somewhat lower concentration of 6 molal has been chosen as it represents a compromise between yielding a strong NDIS contrast and having a larger ratio of water molecules to ions. The NDIS experiment is arguably the most direct method for acquiring information on the solvation structure of a specific ion (assuming isotopes of the nuclei with significantly different coherent neutron scattering lengths are available). Of the many computational studies performed on the chloride ion in aqueous solution, those that compare the MD modeling to the structural measurement are rare,[12] and those that use NDIS data are even rarer.[6] This is mostly because NDIS requires relatively concentrated solutions where ion-ion interactions can play a significant role in the structure of the solution. The ion-ion interactions do not complicate matters only if simulations are performed at low concentrations, consequently, the majority of the chloride models are parameterized on a single ion at infinite dilution on measurables such as enthalpy of hydration (see Ref. [4] and references therein). Many MD studies have been performed with the chloride ion parameters obtained in such a way, including polarizability[13] or within non-polarizable force fields.[14-16]

The validity of the model is ultimately contingent on getting the water-water, solute-water, and solute-solute balance correct. There is, therefore, merit in comparing the simulation and experimental data on solutions with higher solute concentrations, where water-water, solute-water, and solute-solute interactions are all significant factors. This paper tackles exactly this point. NDIS data from a concentrated solution of lithium chloride (with chloride isotope substitution at 6m) is used to examine validity of various models for MD simulations. Specifically we study the relationship between the size and effective polarizability (implemented via charge rescaling[17]) of the chloride ion and its

hydration in a concentrated solution, asking the question which of these parameters yield the best fit to the experimental data. As a next step, we employ MD as an interpretive tool to examine the details of hydration of the chloride ion.

An important point specifically examined in this paper is the relationship between the effective charge of the ion and the structure of the aqueous solution. In empirical force fields, atomic point charges are used to emulate the electrostatic properties of the molecular components.[18] Within non-polarizable simulations, atomic charges for solutes and for the water molecule itself are typically scaled down to fit experimental observables in aqueous solution.[19] This is, however, rarely done with ions,[14,16] even though numerous recent studies suggest that this can have a very large effect on the ion-ion interactions, especially with high charge density ions.[20-22] The dielectric constant of water can be split into a nuclear and electronic contribution, with the effects of the latter explicitly missing for ion-ion interactions in non-polarizable simulations. It has been shown that effective inclusion of this electronic contribution, which for water amounts to $\varepsilon_{el} = 1.78$, is equivalent to scaling the charges of the ions by $(\varepsilon_{el})^{-1/2} = 0.75$. [22-24] As in our previous work, we denote such charge scaling as the electronic continuum correction (ECC).

Methods

Experimental Details

$Na^{35}Cl$ and $Na^{37}Cl$ were obtained from Sigma-Aldrich. Each of these salts were separately placed on a high vacuum line, and H_2SO_4 was slowly added. The HCl gas released was condensed in another flask using liquid nitrogen prior to being dissolved in D_2O. This process yielded ~95% of the distilled isotopic HCl. A solution of known concentration of LiOH was prepared (the natural abundance of lithium isotopes was used), and identical quantities added to two flasks. To one of these a slight excess of $H^{35}Cl$ was added and to the other that of $H^{37}Cl$. In both cases the all the volatile material was removed under vacuum and D_2O added. The D_2O was removed under vacuum and more D_2O was added. This process was repeated 3 times to ensure that both solutions had identical H/D compositions. The final mass of the solutions was ~2000 mg.

Neutron diffraction data was obtained on the D4C diffractometer at the ILL, Grenoble.[25] Data were acquired on each sample for about 8 hours, and then corrected for background, multiple scattering, and attenuation prior to being normalized with respect to a standard vanadium bar. We thus obtained the so-called "total-scattering" diffraction patterns for both solutions S(Q). From the direct difference of these two structure factors, the NDIS first-difference function $\Delta S_{Cl}(Q)$ was obtained. This can be numerically expressed as:

$$\Delta S_{Cl}(Q) = 23.9\, S_{ClD}(Q) + 10.1\, S_{ClO}(Q) + 1.43\, S_{ClCl}(Q) - 0.370\, S_{ClLi}(Q) - 35.4 \qquad (1)$$

The difference function $\Delta S_{Cl}(Q)$ can be Fourier-transformed to give the corresponding real space function:

$$\Delta G_{Cl}(r) = 23.9\, g_{ClD}(r) + 10.1\, g_{ClO}(r) + 1.43\, g_{ClCl}(r) - 0.370\, g_{ClLi}(r) - 35.4 \qquad (2)$$

In each case the prefactors for the g(r)s are calculated using the formula $c_{Cl}c_x\Delta b_{Cl}b_x$ where c is the atomic concentration of the given species, b is the average coherent neutron scattering length of that species, and Δb_{Cl} is the difference in the coherent neutron scattering lengths of ^{35}Cl and ^{37}Cl.

Simulation Details

Classical molecular dynamics simulations were performed for aqueous solutions of 6.0 m LiCl. The LiCl solution contains 144 Li^+ , 144 Cl^- , and 1333 water molecules in a cubic box with a length of 35.54 Å giving the experimental number density of 0.0955 atoms/$Å^3$. These simulations were all run using the SPC/E water[26] and a lithium model previously parameterized on neutron scattering data.[27] The OPLS[28] and Dang.[29] chloride force field were used initially for the chloride ion, hereafter referred to as the large and small chloride based on the respective sizes of their Lennard-Jones σ-parameters. In each case the simulations were run with both full and ECC ionic charges[17,22,23] (charges of +1/-1 or +0.75/-0.75 for the lithium/chloride ion, respectively). Based on these simulations, a refinement was made yielding an intermediate sized chloride force field, hereafter called the medium chloride. The size of the medium chloride was chosen based on a linear extrapolation between the large and small chloride ECC simulations, such that the peak position of the first peak in $\Delta G_{Cl}(r)$

would coincide with the experimental measurement. The medium chloride ECC charges force-fields was also combined with the TIP4P/2005 water model.[30] For each system we collected 30 ns trajectories with a 1fs time step using the Gromacs software.[31] Simulations were performed at a constant volume and temperature of 300 K maintained by a CSVR thermostat[32] with a time constant of 0.5 ps. The geometry of water molecules was kept rigid using the Settle algorithm.[33] 3D periodic boundary conditions were employed with short range electrostatic and van der Waals interactions truncated at 1.2 nm and the long-range electrostatic interactions treated by the particle mesh Ewald method.[34]

Table 1. Force field parameters of ions employed in simulations LiCl aqueous solutions.

	σ (Å)	ε (kJ/mol)	Charge (full/ECC)
Lithium	1.80	0.07647	+1.0 / +0.75
Small Chloride	3.785	0.52162	-1.0 / -0.75
Medium Chloride	4.10	0.4928	-1.0 / -0.75
Large Chloride	4.417	0.4928	-1.0 / -0.75

Results and Discussion

Comparison of Neutron Scattering and Molecular Dynamics results

Thanks to the high contrast of our samples (~35 millibarns), and the excellent counting statistics and instrument stability of the D4C diffractometer,[25] the obtained function $\Delta S_{Cl}(Q)$ had a very good signal to noise ratio (Figure 1). In order that these results could be directly compared with the simulation data a small Placzek correction

was applied.[7] A qualitative perspective of the ion density and degree of ion pairing in these solutions can be obtained from representative snapshots from these simulations (Figure 2). Two snapshots are depicted, one from the small full charges force-field showing an extensive ion pairing, and one from the medium ECC charges force-field which was found to be the best fit to the experimental data. From each simulation the functions $\Delta S_{Cl}(Q)$ and $\Delta G_{Cl}(r)$ were calculated according to equations 1 and 2 and compared to the results of experimental measurements of the same functions (Figures 3 and 4). The calculated functions reveal how the effective charge and size of the ion affects the solvent structure around the chloride ion in molecular dynamic simulations. Of the simulations in this study the medium sized chloride with ECC charges gave the best fit to the experimental data. To better understand the successes and failures of these various chloride models it is necessary to examine the detailed relationship between the structure of these solutions and manifestations thereof in the function $\Delta G_{Cl}(r)$ calculated from the simulations.

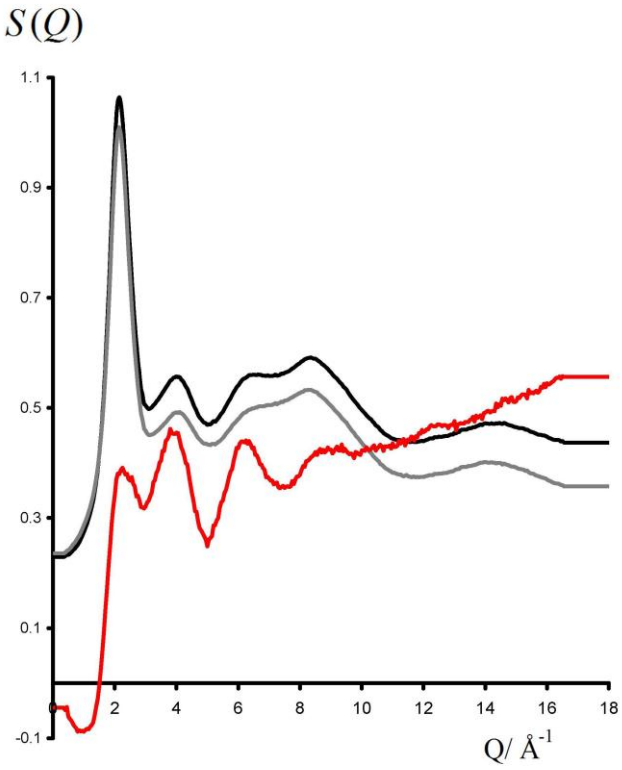

Figure 1. The total scattering patterns S(Q) for 6m $Li^{35}Cl$ (black) and $Li^{37}Cl$ (grey) and the first order NDIS function $\Delta S_{Cl}(Q)$ x7 (red).

The general form of the chloride solvation is similar in all the simulations (Figure 5) with one of the hydrogens of the first solvation shell waters pointing almost directly at the chloride ion, as elucidated earlier from experimental studies on these systems.[6] The first dominant peak at ~2.2 Å in the function $\Delta G_{Cl}(r)$ is, therefore, known to be due to one of the hydrogens of the first shell hydration shell waters (see Figure 5). The position of this first peak is very sensitive to the size of the chloride ion in the simulation (Figure 4), occurring at higher *r* for bigger chloride. In order to test if this peak was sensitive to the LiCl concentration an additional simulation was run using the best force-field (i.e., medium ECC charges), but at 3m instead of 6m. From this simulation the function $\Delta G_{Cl}(r)$ was calculated (Figure 6). As expected, the lower concentration of this solution yielded a lower contrast in the predicted neutron scattering function $\Delta G_{Cl}(r)$ (18.7mb for the 3m solution versus 35.4mb for the 6 m solution). However if the signal was scaled up to the contrast of the 6m solution (scaling by 35.4/18.7), it became clear that the concentration change had almost no effect on the position or shape of the first peak in $\Delta G_{Cl}(r)$.

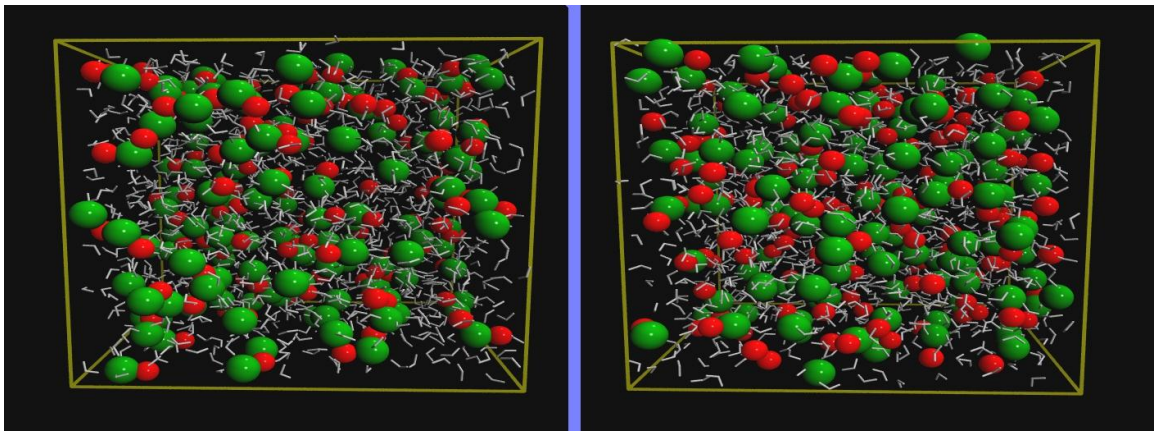

Figure 2. Snapshots of two of the 6m LiCl simulations used in this study. Li^+ ions are shown in red, and Cl^- ions are shown in green. Left: results from the small full charge force field in which almost every lithium ion is paired with a chloride ion. Right: results

from the medium ECC charge force-field which gives the best fit to the experimental data, where there are far less Li-Cl ion pairs.

Changing the charge density on the ion from the full to ECC charges has the effect of moving the first peak in $\Delta G_{Cl}(r)$ to slightly higher *r* and making it slightly broader. It can be shown that this first sharp peak at ~2.2 Å constitutes the majority of the Q-space data above ~ 5 $Å^{-1}$ in $\Delta S_{Cl}(Q)$ with the *r*-space peak position being effectively determined by the wavelength of the Q-space data above ~5$Å^{-1}$. The difference in the first peak positions in $\Delta G_{Cl}(r)$ from the MD and experimental data in Figure 3 can be seen in Q-space data as a phase shift above ~5$Å^{-1}$ in Figure 3. Focusing on the medium chloride ECC charges data, the calculated and experimental peak positions in *r*-space are almost identical, as is the phasing in Q-space. For the small chloride ECC charges, the first peak in *r*-space is shifted to lower *r*, which manifests itself in Q-space by the MD data showing a longer wavelength phasing compared to the experimental data. Conversely, with the larger chloride and ECC charges, this first peak in $\Delta G_{Cl}(r)$ is shifted to higher *r* compared to the experimental data, which can be seen in Q-space by the molecular dynamics data showing a shorter wavelength than the experimental data above about ~ 5 $Å^{-1}$. Only the large full charge and medium ECC charge chloride produce a good fit for the position of this first peak.

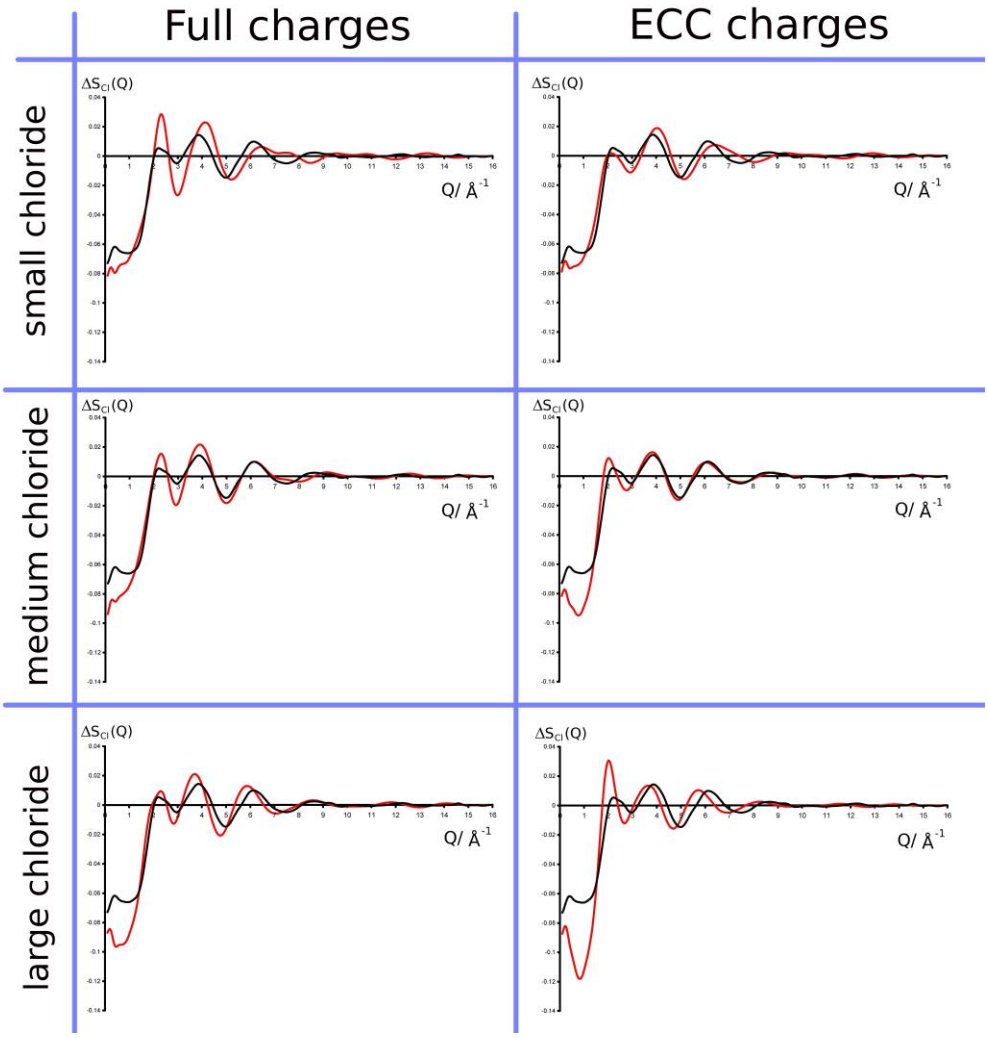

Figure 3. The functions $\Delta S_{Cl}(Q)$ for each of the simulations in this study (red) and the experimental measurement (black). The experimental data has been subjected to a small Placzek correction to remove the background slope on the data.

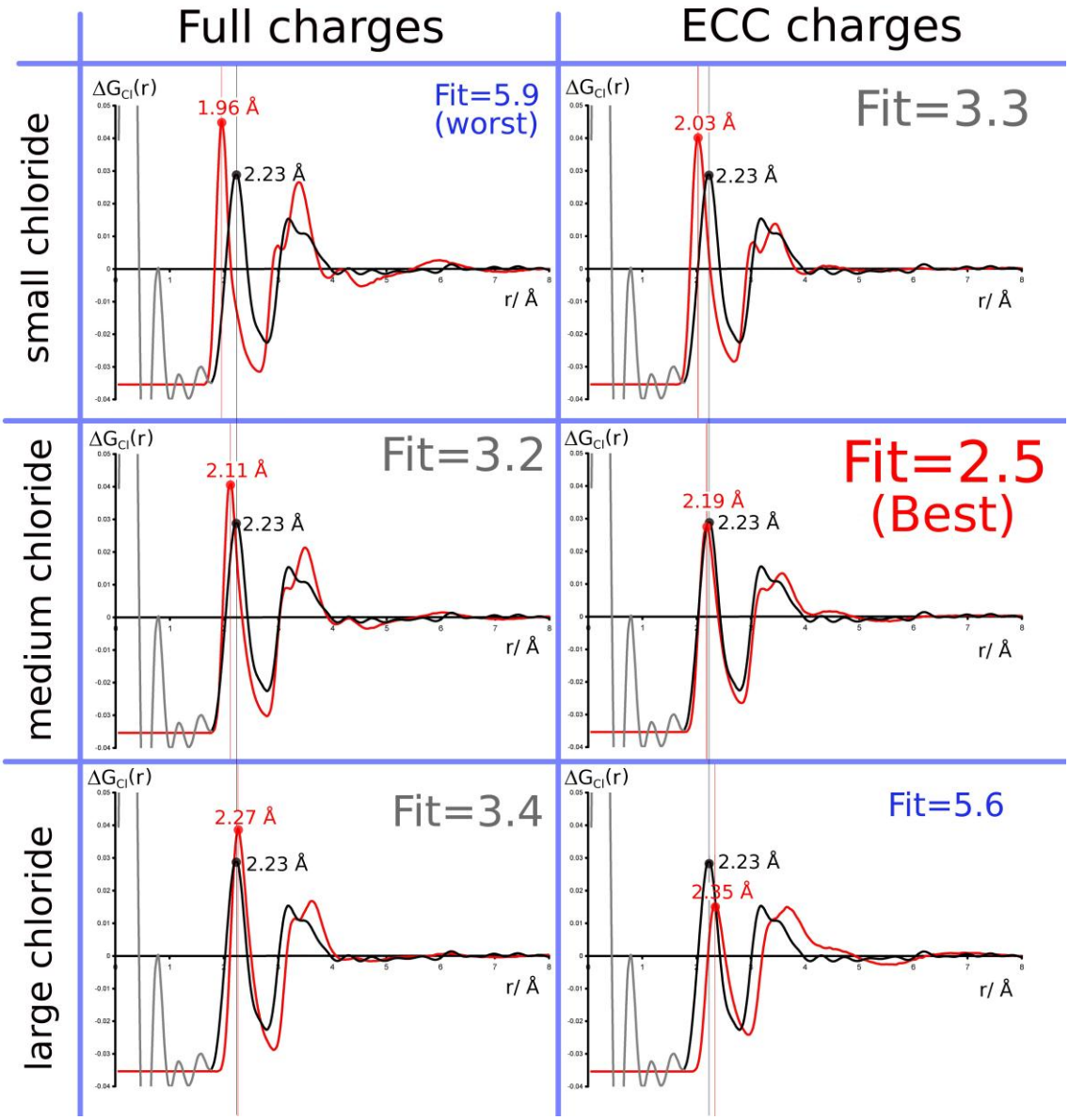

Figure 4. The comparison of the experimental (black) and simulations data (red) for the functions $\Delta G_{Cl}(r)$. In each case the position of the first peak is shown in the appropriate color. With each set of data a 'fit' parameter is shown which is the integral of the absolute values of the differences of the two functions weighted by r^2 (such that the comparison is proportional to coordination number) in the region 1.5 - 6 Å.

The remaining oxygen and hydrogen atoms of the water molecules of the first hydration shell are seen in the function $\Delta G_{Cl}(r)$ as a partially resolved doublet at ~3.5 Å with the lower *r* and higher *r* peaks of this feature being due to the oxygen and hydrogen respectively. Interestingly, in the experimental data the oxygen correlation produces a slightly larger peak than the hydrogen in this partially resolved doublet, while in all of the MD simulation data the opposite is true. Both the *r* and Q-space data are again sensitive to the positions of these features. Here the small and medium ECC charge simulations are the most successful in reproducing both the size and position of this second feature in $\Delta G_{Cl}(r)$. Only the medium ECC charge simulation accurately reproduces both the first and second peak in $\Delta G_{Cl}(r)$.

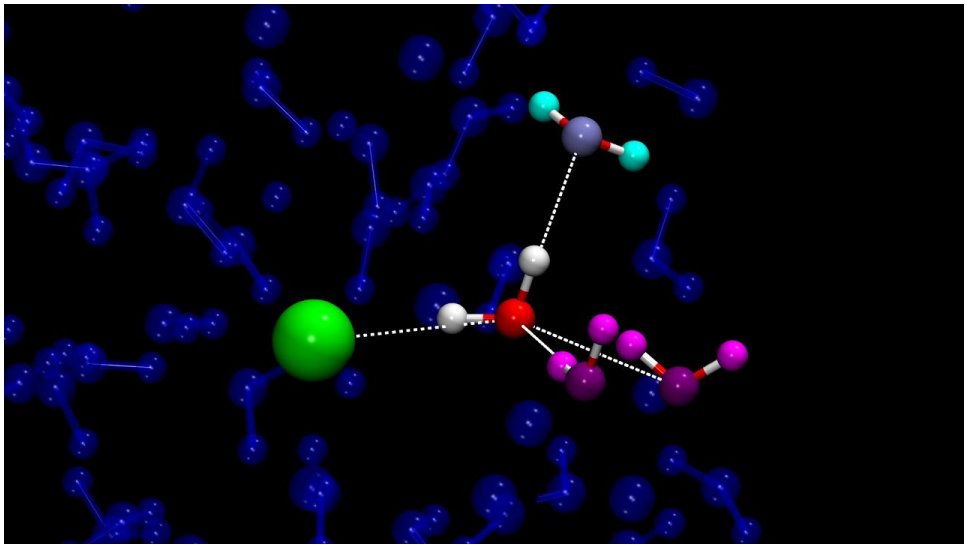

Figure 5. The general structure of the first and second hydration shell of the chloride ion. The first shell (with the oxygen shown in red and hydrogens in white) has the OH bond pointing directly at the chloride ion. The second shell (the three remaining uniquely colored waters) is much more disordered, but generally consists of two waters donating hydrogen bonds to the first shell (shown in purple) and one being an acceptor to the water in the first hydration shell (shown in cyan and grey/blue).

Second hydration shell around chloride

In all of the simulations, the water molecules from the second hydration shell of the chloride ion are directly hydrogen bonded to those from the first shell. The first shell

waters can be the donor of one, and the acceptor of two hydrogen bonds to waters in the second hydration shell (termed hereafter second shell donors and second shell acceptor) (Figure 5). For all the waters in the second hydration shell, the distance between the oxygen and the chloride is roughly the same. The distance to the hydrogens of the second shell donors and acceptors will, however, be different (Figure 5). It is also expected that there will be about twice as many second shell donors as there are second shell acceptors. The best way of seeing such correlations is to dissect the function $\Delta G_{Cl}(r)$ as calculated from the MD simulations into its components $g_{ClH}(r)$, $g_{ClO}(r)$, $g_{ClCl}(r)$, and $g_{ClLi}(r)$ (Figure 7). The $g_{ClO}(r)$ component is a good indicator of the level of structure (sharpness), and position of the first and second hydrations shell. In each case as the ion becomes larger, the first peak in $g_{ClO}(r)$ moves to higher *r*, while simultaneously becoming broader, with less evidence for a second hydration shell. Similarly, in each case going from full to ECC charges has the effect of the hydration shell moving to a slightly higher *r* and becoming broader. As the size of the ion increases, so the peaks for the first and second shell become less well defined (see the $g_{ClH}(r)$ and $g_{ClO}(r)$ components in Figure 7), however in $\Delta G_{Cl}(r)$ for ECC simulations there is an increasing oscillation in the region 4 - 6 Å (Figure 4). This is actually due to a rather subtle phenomenon where even though the smaller ion has a more structured second hydration shell (based on $g_{ClO}(r)$), in the function $\Delta G_{Cl}(r)$ this structure is hidden by the complementary nature with the $g_{ClH}(r)$ component. There are previous examples in the literature where g(r) serves as a poor proxy for the three dimensional structures in water. Namely, an earlier study has made a comparison between TIP3P and TIP4P water models based on the function $g_{OO}(r)$.[35] Even though TIP3P and TIP4P have very similar three dimensional structures, TIP3P does not have a second peak in $g_{OO}(r)$ while TIP4P does.

The observation that relatively minor changes in the three dimensional structure of the solution can lead to a significant differences in the function $\Delta G_{Cl}(r)$ at higher *r* means that getting an exact fit between the experimental and simulation data is less critical in this region. From these observations it can also be deduced that the second hydration shell will be more sensitive than the first one to the choice of water model, as this is far more dependent on water-water hydrogen bonding than the first hydration shell.

To examine this, the force-field that gave the best fit to the experimental data (medium ECC charges) was rerun using the TIP4P 2005 rather than the SPC/E water model. We found that there was relatively little change to the features related to the first hydration shell, but larger changes were visible in the second hydration shell region (Figure 8 and Table 2). Previous studies similarly showed that the position of the first hydration shell peaks does not depend greatly on the water model employed in the simulations.[4,14]

Local concentrations of water and lithium around the chloride ion

The metrics chosen to assess ion pairing in the investigated systems was based on local concentrations. A cut-off of 4 Å was chosen as it roughly constitutes the position of the first minimum after the first maximum of the radial distribution function $g_{ClO}(r)$, see Figure 8. This *r* range also accounted for all the lithium ions in direct contact with the chlorides. The coordination numbers of both Li^+ and O within 4 Å from the chloride for each of these simulations are shown in Table 2. Local concentrations were calculated from the ratio of Li^+ to water oxygen atoms. Almost all of these solutions show a depletion (compared to bulk solution concentration) of Li^+ around the chloride ion. When the effective charges (+/-0.75) are used rather than the full charges (+/-1.0), the local concentration of Li^+ decreases by a factor of about two. The effect is somewhat reversed when the size of the chloride ion is decreased. The decrease in the local concentration is almost entirely due to fewer counterions in the first hydration shell as the number of water molecules appears to have a rather small dependence on the size of the ion. Our observation that even for monovalent ions with a relatively low charge density, such as chloride, pairing with counterions is rather sensitive to the (effective) charge and the size of the ion has implications for studies of ion-ion interactions in proteins. Previous studies have indeed suggested that these factors may represent a significant factor in accurately modeling the strength of salt bridges in proteins.[22]

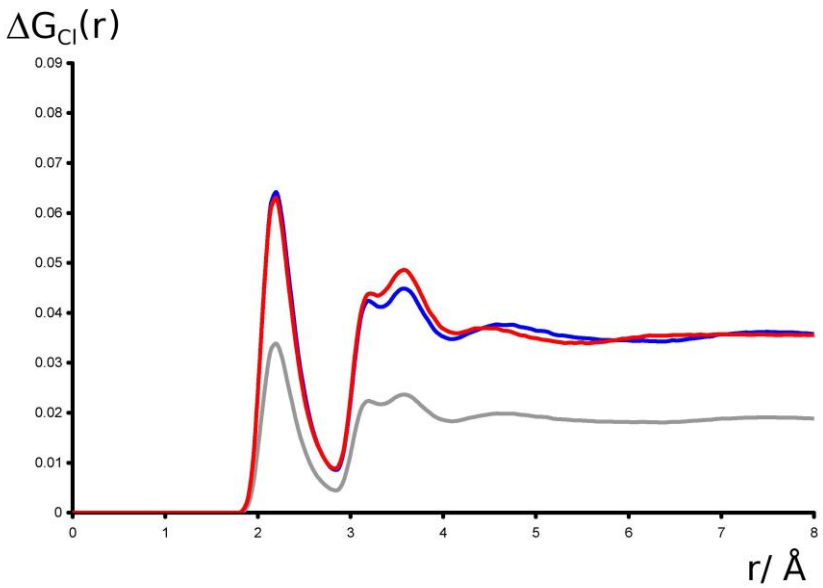

Figure 6. The functions $\Delta G_{Cl}(r)$ as predicted from the medium ECC charge simulation for 3m (grey) and 6m LiCl (red). Due to the difference in the concentration of these two solutions there is only about half the contrast expected for the 3m solution as for the 6m solution. When the contrast of the 3m solution (18.7mb) is scaled up to that of the 6 m solution (35.4mb, blue) it can be seen that there is little dependence of the first hydration shell on concentration in this range.

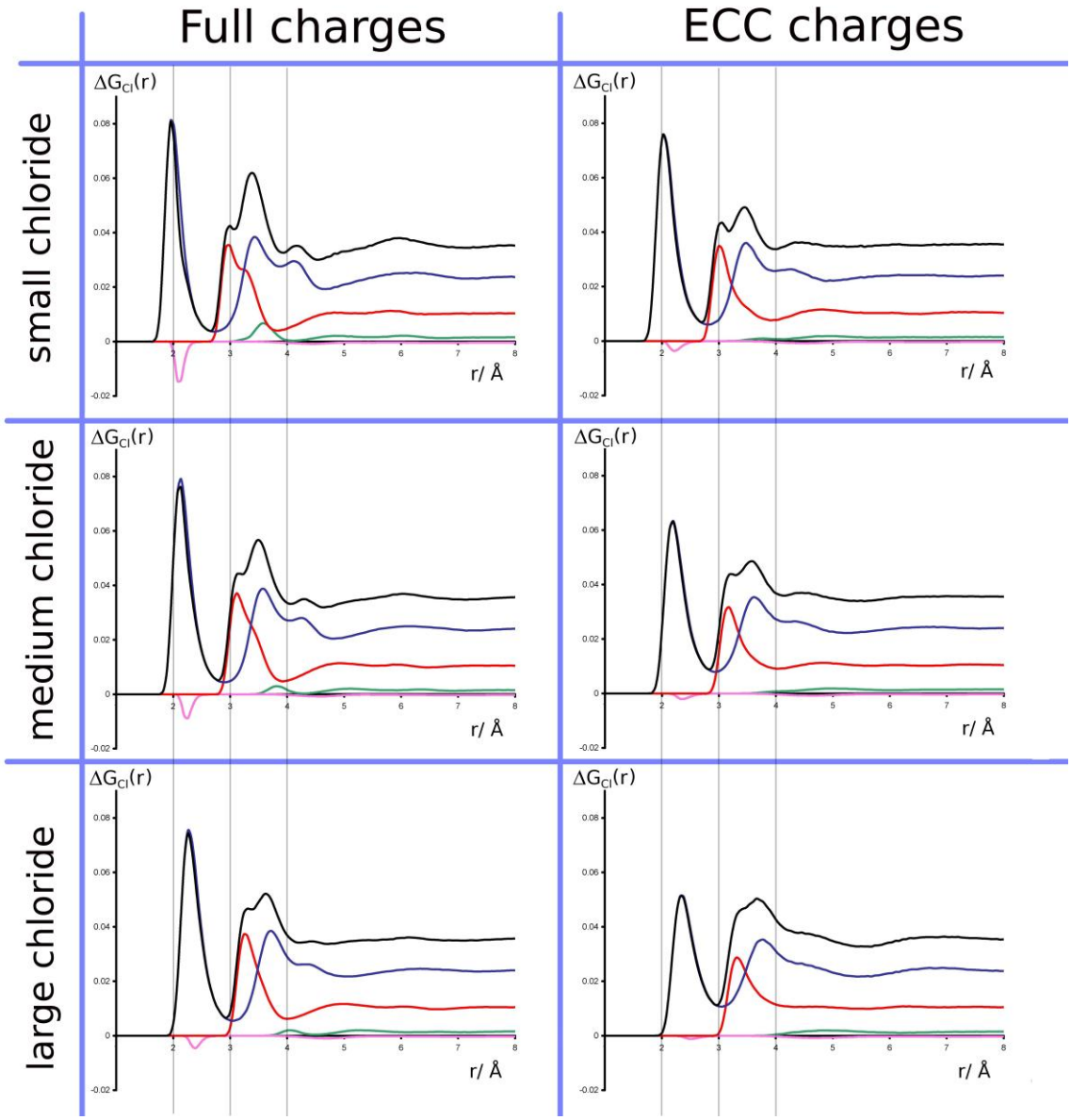

Figure 7. The difference function $\Delta G_{Cl}(r)$ as calculated from the various simulations in this study (black). In each case the components of this function from the Cl-H, Cl-O, Cl-Li, and Cl-Cl correlations are shown in blue, red, pink, and green respectively.

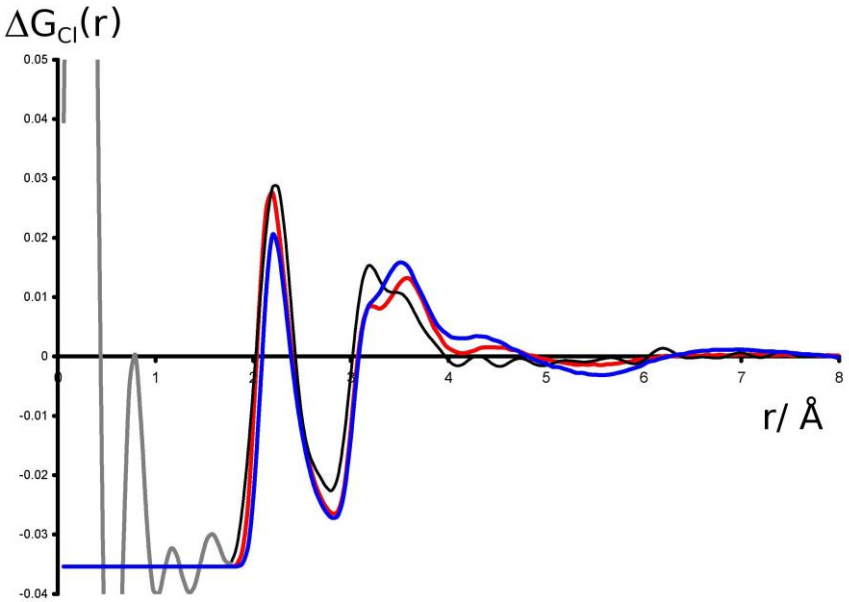

Figure 8. Comparison of the experimental (black) and simulations data using the medium charges ECC force-field using SPC/E water (red) and TIP4P 2005 (blue) for the function $\Delta G_{Cl}(r)$.

Hydration number of the chloride ion in concentrated solutions

Integrating up to a fixed value in *r* space is a reasonable method for establishing the mass balance of what is in contact with the chloride ion (between about 7.5 and 8 waters molecules and between 0.4 and 1.4 lithium ions), but it discards a lot of the detailed information about the hydration of the chloride ion available from the simulations. This raises an interesting question: Does integrating $g_{ClO}(r)$ for these functions up to a certain r value give a well-defined hydration number[36] and, if yes, how does it depend on the chloride size and effective charge? To answer this question, for each simulation the nearest seven water oxygens were tagged and the contribution of each of those oxygens to the function $g_{ClO}(r)$ and hydrogens to $g_{ClH}(r)$ were evaluated (Figure 7). This figure offers a deeper insight into the differences in the hydration patterns of these chloride models. In each case the first 5 water molecules are shown in grey with the contributions from the 6th and 7th water molecules (which are completing the first solvation shell around chloride) to the functions $g_{ClO}(r)$ or $g_{ClH}(r)$ highlighted in red and blue, respectively. The full charge models have sharper peaks in $g_{ClO}(r)$ for both

the 6^{th} and 7^{th} water relative to the ECC charges models. The size of the chloride appears to have relatively little effect on the form of the 6^{th} and 7^{th} waters beyond shifting their peaks to somewhat higher *r*. Larger differences are seen in the hydrogens contributing to the function $g_{ClH}(r)$. With the ECC charges, in each case the 6^{th} water is ordered, while the 7^{th} water has no significant contributions to the first peak in $g_{ClH}(r)$. However with the full charges model, generally both the 6^{th} and 7^{th} waters have peaks that contribute to the first peak in $g_{ClH}(r)$. The exception here is the small chloride model which does not appear to provide enough room for the 7^{th} water molecule. The contributions of the second hydrogen of a given water molecule to the function $g_{ClH}(r)$ in the region 3 - 4.5 Å gives an idea of the angular ordering of the waters in the first hydration shell. In this second peak region it is universally found that a higher charge density on the chloride in full charge models leads to significantly stronger ordering of the first hydration shell waters than within the corresponding ECC charge models. These results are suggestive that changing the effective charge from -1.0 to -0.75 has a larger effect on the hydration of the ion than reducing the VDW radii by ~ 10%.

Table 2. The coordination numbers of the chloride ion in the various simulations out to a distance of 4.0 Å

	Small full	Medium full	Large full	Small ECC	Medium ECC	Large ECC	TIP4P Medium ECC
Oxygen	8.0	8.1	8.0	7.7	7.7	7.6	7.7
Lithium	1.4	0.85	0.80	0.74	0.54	0.39	0.83
Local concentration of Li^+ (molal)	9.6	5.9	5.5	5.4	3.9	2.9	6.0

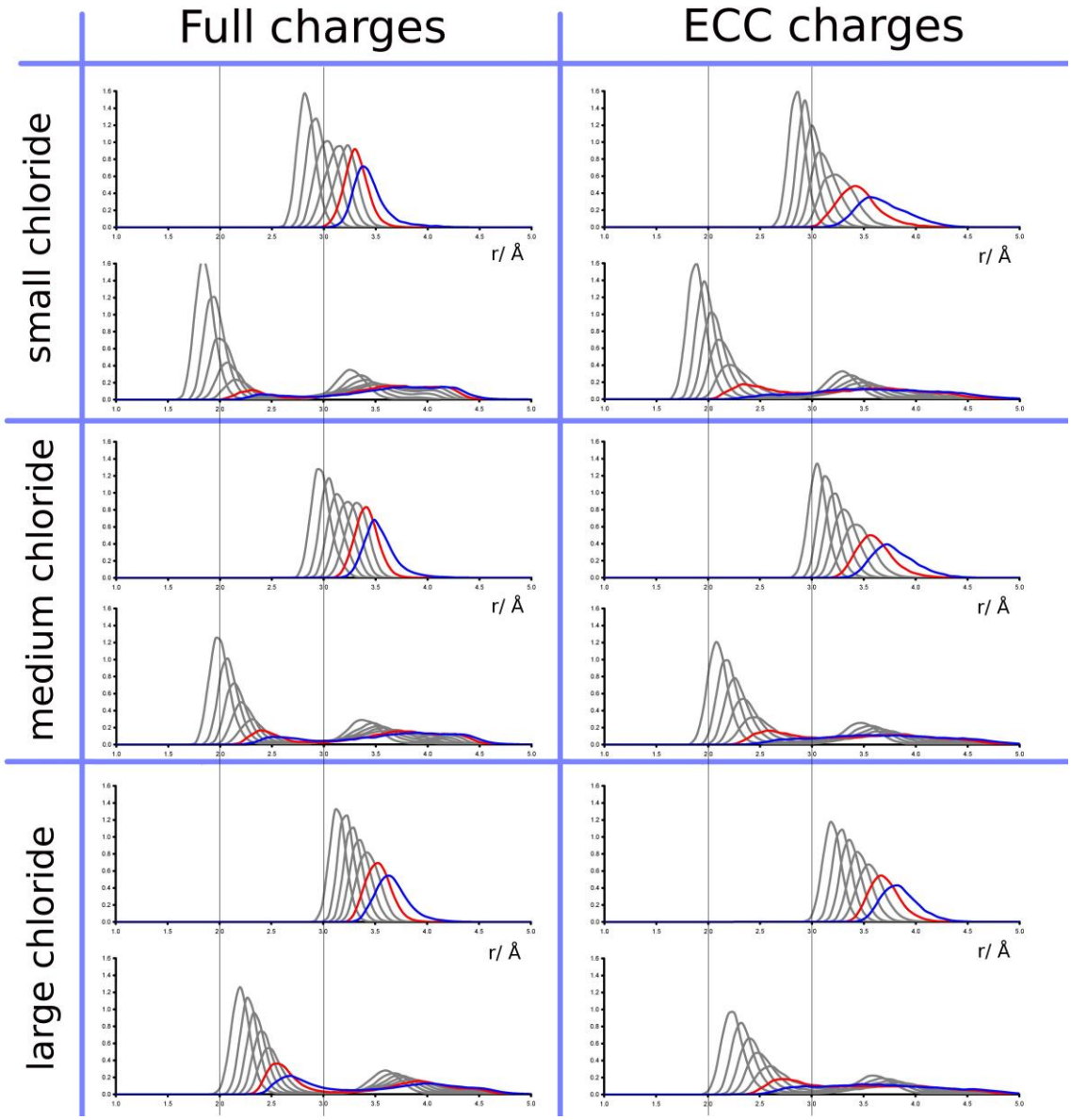

Figure 6. The radial distribution functions for the first 7 water molecules (selected by Cl-O distance) around the chloride ion. In each case, the upper plot shows the g(r) for the water oxygen, while the lower plot depicts the g(r) for the two hydrogens on that water molecule. The first 5 waters are shown in grey with the 6th and 7th waters shown in red and blue, respectively.

Conclusions

Neutron scattering experiments and molecular dynamics simulations were performed on concentrated aqueous solutions of lithium chloride in order to examine the

solvation of the chloride ion. This system was chosen as a direct challenge to the simulation data in a situation where the ion-water, ion-ion, and water-water interactions are all important. The good signal to noise ratio in the experimental neutron scattering data produced here gave a very stringent constraint on the position of the first peak the function $\Delta G_{Cl}(r)$. The force-fields in this study had ion sizes that varied by ~20 %, and were performed with both full and ECC charges on the ions. The fit between the MD and experimental data could easily identify the more and less successful force-fields. As with previous studies it was found that in order to obtain a good fit between the experimental and simulation data the correct ion size and charge density was required. The medium sized ECC charge chloride force-field provided a significantly better fit to this experimental data than all of the other force-fields examined in this study. This is in line with our previous studies of concentrated aqueous solutions of Gdm_2CO_3,[21] KNO_3/K_2CO_3 [20] and Li_2SO_4/LiCl (examining the solvation of the Li^+ ion),[27] which showed that ECC charges gave a significantly better fit to the experimental data than the more conventional full charge force fields. The present results support a suggestion that scaled ionic charges charges, which effectively take into account polarization effects, could be used in MD simulations to improve description of solutions (particularly concentrated ones) even in cases where the ion has a relatively low charge density, such as is the case for the chloride ion.

ACKNOWLEDGMENT

We thank George Neilson for valuable comments and P.E.M. thanks S. Rempe and S. Ansell for aiding in the planning stages of this study. We also thank the ILL and its staff for the use of the experimental facilities and allocated beamtime. Support from the Czech Science Foundation (grant P208/12/G016) is gratefully acknowledged. P.J. thanks the Academy of Sciences for the Praemium Academie award. E. P. acknowledges support from the International Max Planck Research School on Dynamical Processes in Atoms, Molecules, and Solids. The access to computing and storage facilities owned by parties and projects contributing to the National Grid Infrastructure MetaCentrum, provided

under the program "Projects of Large Infrastructure for Research, Development, and Innovations" (LM2010005) is appreciated.

References

[1]J. W. Morgan and E. Anders, *Proceedings of the National Academy of Sciences of the United States of America-Physical Sciences* **77** (12), 6973 (1980).

[2]J. Lyman and R. H. Fleming, *Journal of Marine Research* **3** (2), 134 (1940).

[3]L. Petit, R. Vuilleumier, P. Maldivi, and C. Adamo, *Journal of Chemical Theory and Computation* **4** (7), 1040 (2008).

[4]I. S. Joung and T. E. Cheatham, *Journal of Physical Chemistry B* **112** (30), 9020 (2008).

[5]K. Yamanaka, M. Yamagami, T. Takamuku, T. Yamaguchi, and H. Wakita, *Journal of Physical Chemistry* **97** (41), 10835 (1993).

[6]D. H. Powell, G. W. Neilson, and J. E. Enderby, *Journal of Physics-Condensed Matter* **5** (32), 5723 (1993).

[7]S. Ansell, A. C. Barnes, P. E. Mason, G. W. Neilson, and S. Ramos, *Biophysical Chemistry* **124** (3), 171 (2006).

[8]G. W. Neilson, P. E. Mason, S. Ramos, and D. Sullivan, *Philosophical Transactions of the Royal Society a-Mathematical Physical and Engineering Sciences* **359** (1785), 1575 (2001).

[9]G. W. Neilson and J. E. Enderby, *Proceedings of the Royal Society of London Series a-Mathematical Physical and Engineering Sciences* **390** (1799), 353 (1983); S. Ansell, R. H. Tromp, and G. W. Neilson, *Journal of Physics-Condensed Matter* **7** (8), 1513 (1995); P. S. Salmon and G. W. Neilson, *Journal of Physics-Condensed Matter* **1** (31), 5291 (1989).

[10]S. Ansell, J. DupuyPhilon, J. F. Jal, and G. W. Neilson, *Journal of Physics-Condensed Matter* **9** (42), 8835 (1997); A. C. Barnes, J. E. Enderby, J. Breen, and J. C. Leyte, *Chemical Physics Letters* **142** (5), 405 (1987); T. W. N. Bieze, R. H. Tromp, J. R. C. Vandermaarel, Mhjm Vanstrien, M. C. Bellissentfunel, G. W. Neilson, and J. C. Leyte, *Journal of Physical Chemistry* **98** (16), 4454 (1994); J. E. Wilson, S. Ansell, J. E. Enderby, and G. W. Neilson, *Chemical Physics Letters* **278** (1-3), 21 (1997).

[11]I. Howell and G. W. Neilson, *Journal of Physics-Condensed Matter* **8** (25), 4455 (1996); R. H. Tromp, G. W. Neilson, and A. K. Soper, *Journal of Chemical Physics* **96** (11), 8460 (1992); A. P. Copestake, G. W. Neilson, and J. E. Enderby, *Journal of Physics C-Solid State Physics* **18** (22), 4211 (1985).

[12]A. K. Soper and K. Weckstrom, *Biophysical Chemistry* **124** (3), 180 (2006); I. Harsanyi and L. Pusztai, *Journal of Chemical Physics* **137** (20), 204503 (2012); I. Harsanyi, L. Temleitner, B. Beuneu, and L. Pusztai, *Journal of Molecular Liquids* **165**, 94 (2012); I. Harsanyi, P. A. Bopp, A. Vrhovsek, and L. Pusztai, *Journal of Molecular Liquids* **158** (1), 61 (2011); F. Bruni, S. Imberti, R. Mancinelli, and M. A. Ricci, *Journal of Chemical Physics* **136** (6), 064520 (2012); R. Mancinelli, A. Botti, F. Bruni, M. A. Ricci, and A. K. Soper, *Journal of Physical Chemistry B* **111** (48), 13570 (2007); S. Tazi, J. J. Molina, B. Rotenberg, P. Turq, R. Vuilleumier, and M. Salanne, *Journal of Chemical Physics* **136** (11) (2012).

[13]S. J. Stuart and B. J. Berne, *Journal of Physical Chemistry* **100** (29), 11934 (1996); G. Lamoureux and B. Roux, *Journal of Physical Chemistry B* **110** (7), 3308 (2006).

[14]K. P. Jensen and W. L. Jorgensen, *Journal of Chemical Theory and Computation* **2** (6), 1499 (2006).
[15]S. Weerasinghe and P. E. Smith, *Journal of Chemical Physics* **119** (21), 11342 (2003).
[16]M. B. Gee, N. R. Cox, Y. F. Jiao, N. Bentenitis, S. Weerasinghe, and P. E. Smith, *Journal of Chemical Theory and Computation* **7** (5), 1369 (2011).
[17]I. V. Leontyev and A. A. Stuchebrukhov, *Journal of Chemical Physics* **130** (8) (2009).
[18]A. Rahman and Stilling.Fh, *Journal of Chemical Physics* **55** (7), 3336 (1971).
[19]O. Guvench, S. S. Mallajosyula, E. P. Raman, E. Hatcher, K. Vanommeslaeghe, T. J. Foster, F. W. Jamison, and A. D. MacKerell, *Journal of Chemical Theory and Computation* **7** (10), 3162 (2011); A. D. MacKerell, D. Bashford, M. Bellott, R. L. Dunbrack, J. D. Evanseck, M. J. Field, S. Fischer, J. Gao, H. Guo, S. Ha, D. Joseph-McCarthy, L. Kuchnir, K. Kuczera, F. T. K. Lau, C. Mattos, S. Michnick, T. Ngo, D. T. Nguyen, B. Prodhom, W. E. Reiher, B. Roux, M. Schlenkrich, J. C. Smith, R. Stote, J. Straub, M. Watanabe, J. Wiorkiewicz-Kuczera, D. Yin, and M. Karplus, *Journal of Physical Chemistry B* **102** (18), 3586 (1998); Y. Duan, C. Wu, S. Chowdhury, M. C. Lee, G. M. Xiong, W. Zhang, R. Yang, P. Cieplak, R. Luo, T. Lee, J. Caldwell, J. M. Wang, and P. Kollman, *Journal of Computational Chemistry* **24** (16), 1999 (2003).
[20]P. E. Mason, E. Wernersson, and P. Jungwirth, *Journal of Physical Chemistry B* **116** (28), 8145 (2012).
[21]Mario Vazdar, Pavel Jungwirth, and Philip E. Mason, *The Journal of Physical Chemistry B* **117** (6), 1844 (2012).
[22]I. V. Leontyev and A. A. Stuchebrukhov, *Journal of Chemical Theory and Computation* **6** (10), 3153 (2010).
[23]I. Leontyev and A. Stuchebrukhov, *Physical Chemistry Chemical Physics* **13** (7), 2613 (2011); I. V. Leontyev and A. A. Stuchebrukhov, *Journal of Chemical Theory and Computation* **6** (5), 1498 (2010).
[24]M. Soniat and S. W. Rick, *Journal of Chemical Physics* **137** (4) (2012).
[25]H. E. Fischer, G. J. Cuello, P. Palleau, D. Feltin, A. C. Barnes, Y. S. Badyal, and J. M. Simonson, *Appl. Phys. A-Mater. Sci. Process.* **74**, S160 (2002).
[26]H. J. C. Berendsen, J. R. Grigera, and T. P. Straatsma, *Journal of Physical Chemistry* **91** (24), 6269 (1987).
[27]E. Pluharova, P. E. Mason, and Jungwirth P., *Journal of Physical Chemistry* (DOI: 10.1021/jp402532e), in press. .
[28]Jorgensen Wl, (Yale University, 1996).
[29]L. X. Dang, J. E. Rice, J. Caldwell, and P. A. Kollman, *Journal of the American Chemical Society* **113** (7), 2481 (1991).
[30]J. L. F. Abascal and C. Vega, *Journal of Chemical Physics* **123** (23), 234505 (2005).
[31]B. Hess, C. Kutzner, D. van der Spoel, and E. Lindahl, *Journal of Chemical Theory and Computation* **4** (3), 435 (2008).
[32]G. Bussi, D. Donadio, and M. Parrinello, *Journal of Chemical Physics* **126** (1), 014101 (2007).
[33]S. Miyamoto and P. A. Kollman, *Journal of Computational Chemistry* **13** (8), 952 (1992).

[34]U. Essmann, L. Perera, M. L. Berkowitz, T. Darden, H. Lee, and L. G. Pedersen, *Journal of Chemical Physics* **103** (19), 8577 (1995).
[35]P. E. Mason and J. W. Brady, *Journal of Physical Chemistry B* **111** (20), 5669 (2007).
[36]S. Varma and S. B. Rempe, *Biophysical Chemistry* **124** (3), 192 (2006).